

Structural Controls on Postseismic Deformation Following the Mw 7.8 Pedernales, Ecuador Megathrust Earthquake: Insights from Joint Tomographic Inversion and Aftershock Relocation

Mariah Hoskins¹, Anne Meltzer¹, Josh Stachnik¹, Hans Agurto-Detzel², Alexandra Alvarado³, Susan Beck⁴, Philippe Charvis², Yvonne Font², Stephen Hernandez⁵, Clinton Koch⁴, Sergio Leon Rios⁶, Colton Lynner⁴, Marc Regnier⁷, Andreas Rietbrock⁶, and Mario Ruiz⁵

¹Lehigh University

²Géoazur - Université Nice Sophia Antipolis

³Instituto Geofísico de la Escuela Politécnica Nacional

⁴University of Arizona

⁵Escuela Politécnica Nacional

⁶Karlsruhe Institute of Technology

⁷Géoazur - Université Côte d'Azur - IRD - CNRS - Observatoire de la côte d'Azur

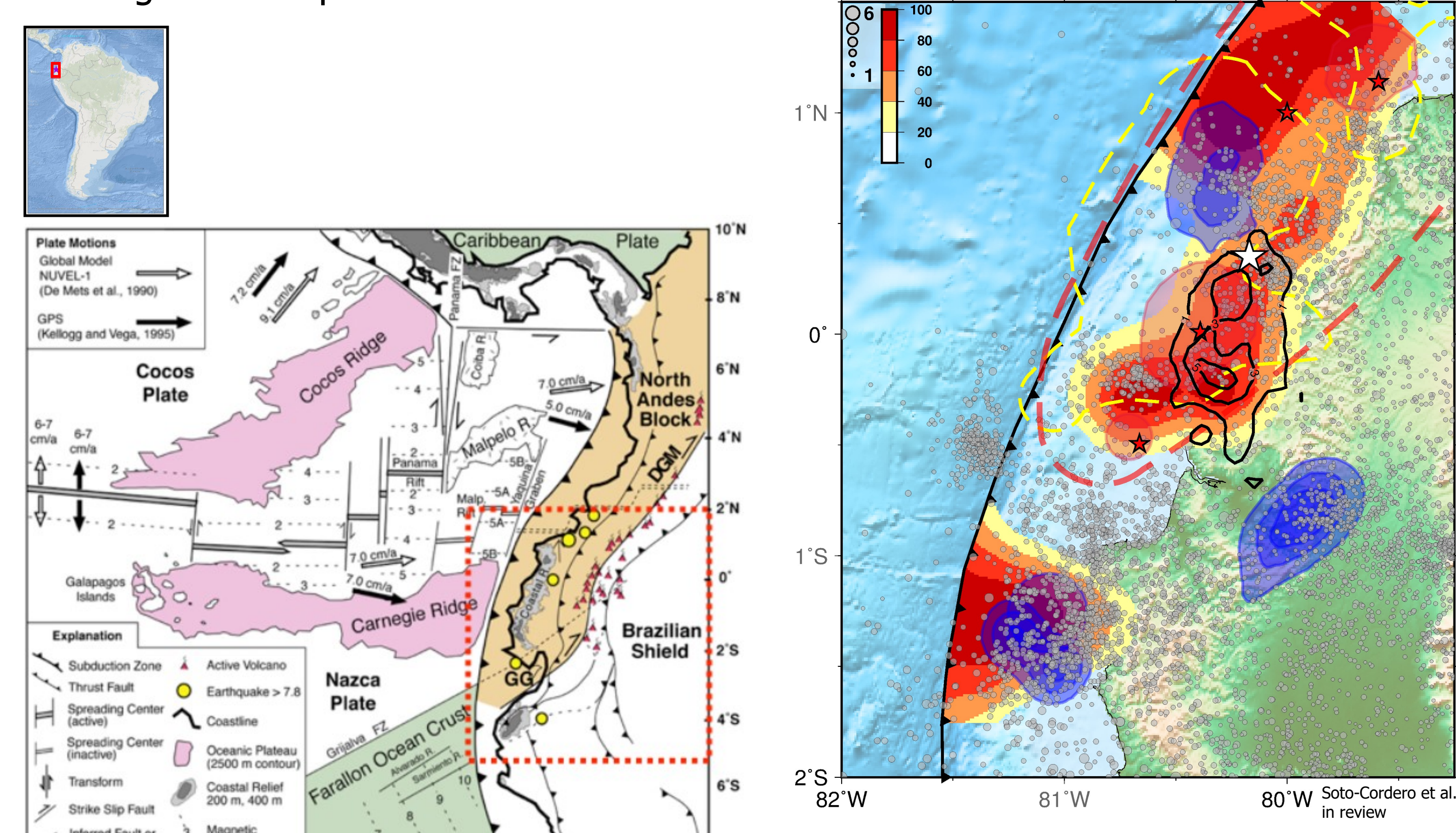
November 23, 2022

Abstract

The north Ecuador subduction zone exhibits segmentation and clustering of seismicity through megathrust, interseismic, and aftershock seismicity. In 1906, a Mw 8.8 megathrust event ruptured a 500 km segment, portions of which were re-ruptured in '42 (Mw 7.8), '58 (Mw 7.7), '79 (Mw 8.2) and 2016 (Mw 7.8 Pedernales event). Segmentation between the ruptures is caused in part by subducting topography and upper plate structure. Upper plate structure in north Ecuador includes major faults, sedimentary basins and accreted terranes. An international aftershock deployment and the Ecuador permanent network (RENSIG) recorded aftershocks of the 2016 Pedernales event. We performed finite difference tomography in a joint inversion for 3D velocity and earthquake location, using body wave arrivals of aftershocks. The Manabi, Manta-Jama and Borbon sedimentary basins are observed as high V_p/V_s features with the Manabi basin seen as a low V_p and V_s feature. High V_p and V_s are associated with accreted forearc terranes. Relocation of aftershocks in the 3D velocity results in previously described “bands” of seismicity collapsing to smaller clusters ranging from ~8-40 km across. South of the rupture area, a cluster near Manabi collapsed landward, and a cluster appeared west of the trench. Three clusters between the trench and directly south of the rupture contain lower plate and plate interface events. The cluster within the rupture area between the patches of greater slip became more focused, and a cluster became defined on the north side of the northern patch of slip. Two clusters outline subducting Atacames seamounts, with events in the lower plate and interface beneath and in front of the seamounts. North of the rupture, the clusters offshore and onshore near Galera contain mostly interface with some upper plate events. The onshore cluster focused around major faults in a transition from north/south to northeast/southwest structures along the coastal range. Events in the cluster near Atacames relocated mainly in the upper plate, and events in the cluster near Esmeraldas remained in the upper plate. Interseismic events cluster in the same locations as aftershock events. Existing features including upper plate structure and subducting features control and focus both postseismic and interseismic deformation across megathrust cycles.

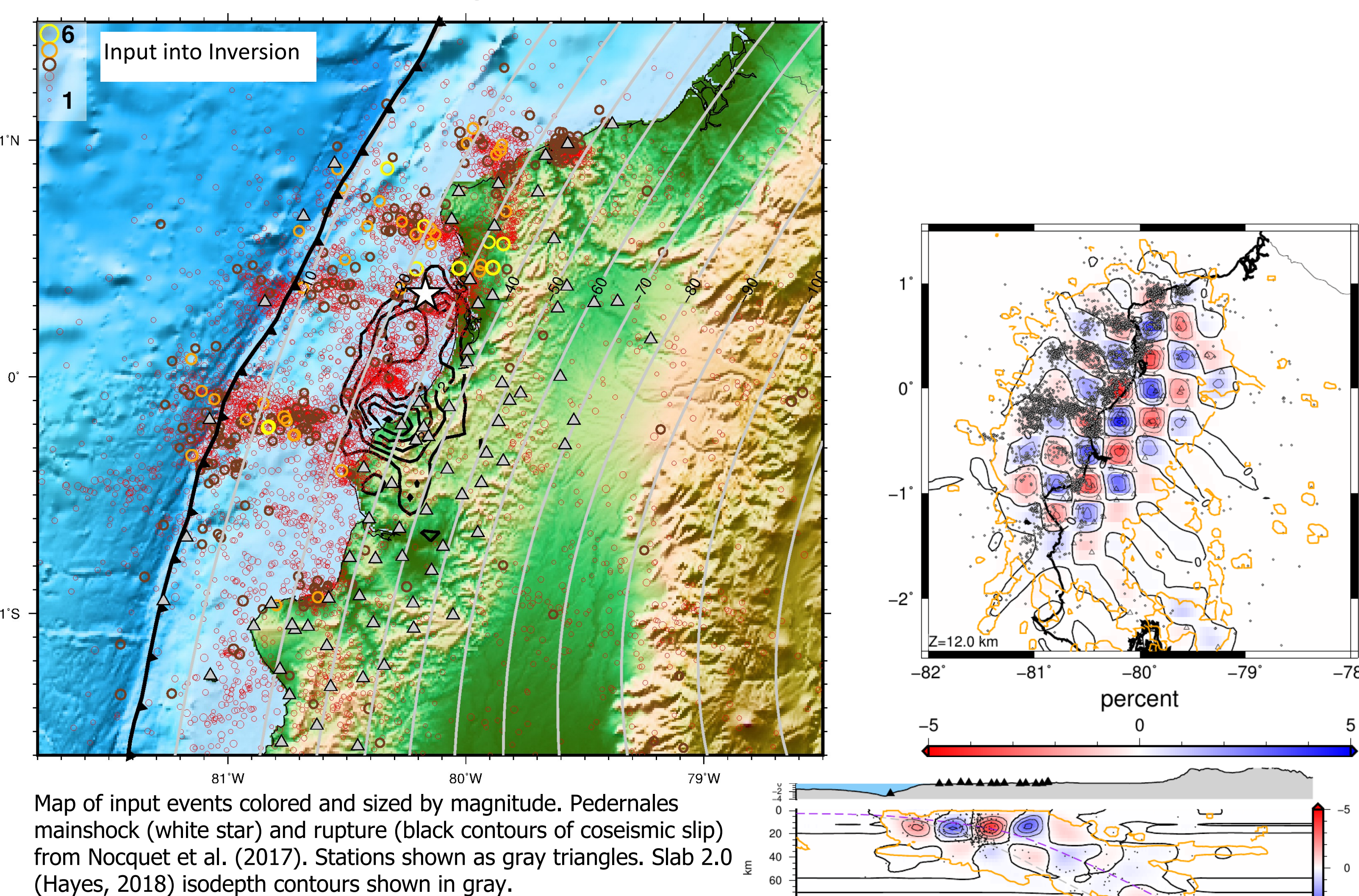
1. Seismo-tectonic Setting of North Ecuador

The north Ecuador subduction zone exhibits segmentation in megathrust ruptures and clustering of seismicity through interseismic and aftershock seismicity. In 1906, a Mw 8.8 megathrust event ruptured a 500 km segment, portions of which were re-ruptured in 1942 (Mw 7.8), 1958 (Mw 7.7), 1979 (Mw 8.2) and 2016 (Mw 7.8 Pedernales event). Segmentation between the ruptures is caused by subducting topography and upper plate structure. Upper plate structure in north Ecuador includes major faults, sedimentary basins and accreted terranes. We perform finite difference tomography using aftershocks recorded following the 2016 Pedernales earthquake to investigate the structures controlling the clustering of seismicity and the megathrust rupture in North Ecuador.



- Variation in plate coupling (white to red) (Chlieh et al. 2014)
- Slow slip identified by GPS (blue shading) (Rolandone et al. 2018)
- Subduction zone
- Carnegie Ridge
- Spreading ridges
- Volcanic arc
- Historic megathrust ruptures (red ellipses, red dashed line) and aftershock areas (yellow dashed lines) (Kelleher, 1972; Mendoza and Dewey, 1984; Swenson and Beck, 1996)
- Pedernales rupture (solid black lines) (Nocquet et al. 2017)
- Interseismic seismicity (Beauval, et al., 2013; IGEPN)

2. Data and Tomographic Inversion Methods



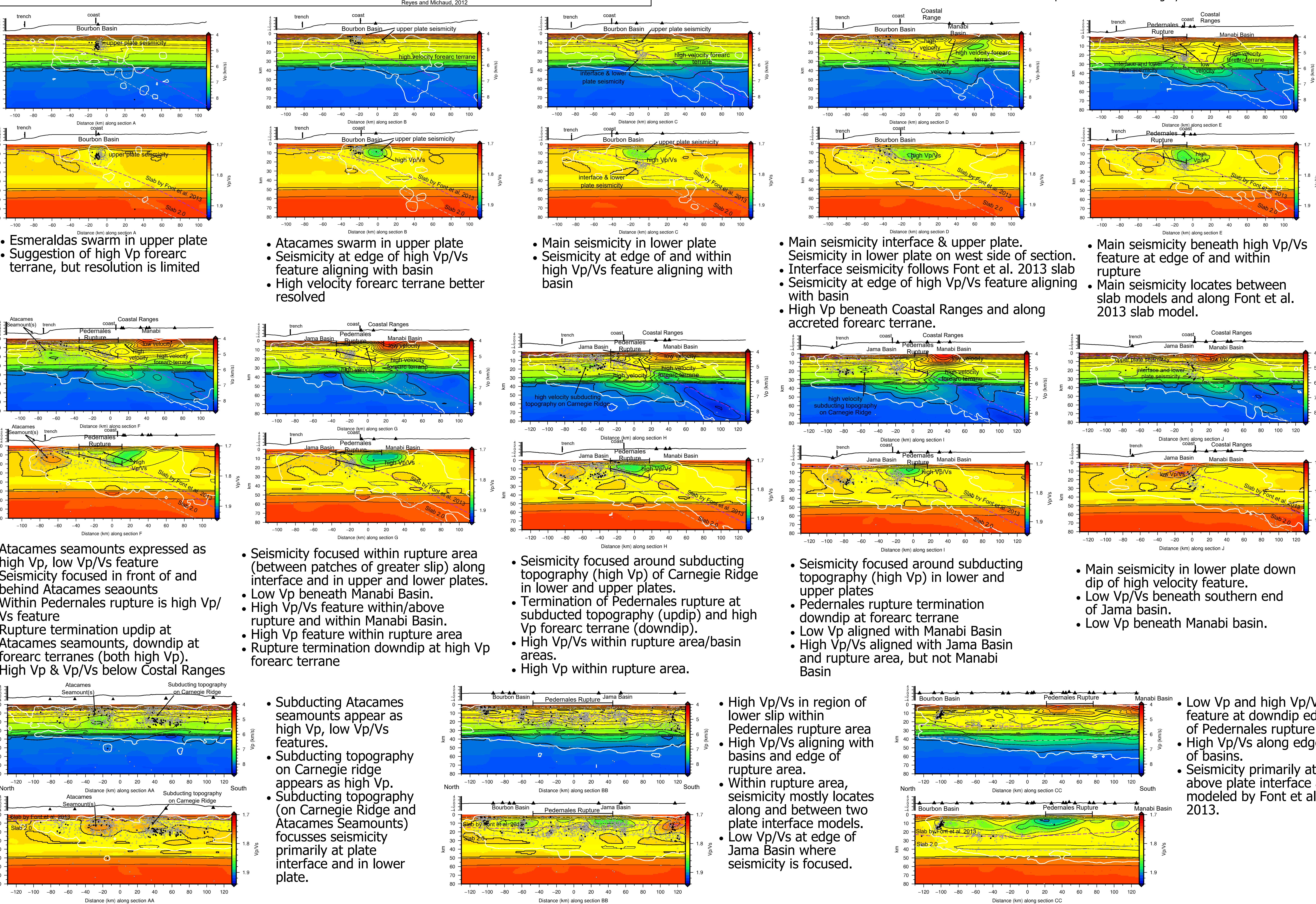
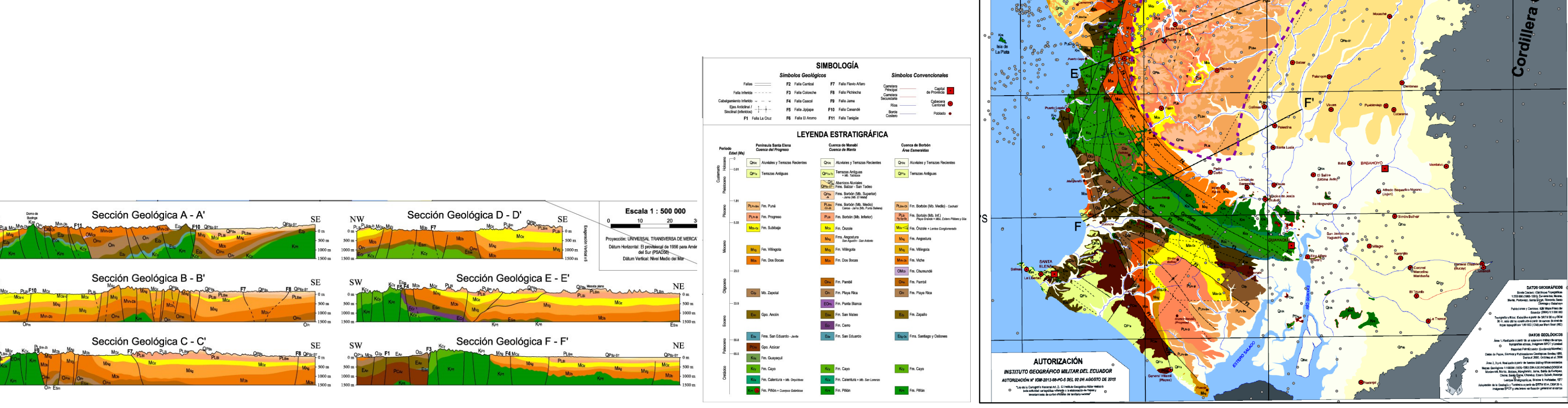
- Method
- Joint inversion for earthquake relocation and 3D velocity model
 - Finite difference tomography method of Roecker et al. (2006)

- Data
- Aftershocks recorded by Ecuador national network (RENSIG) and international aftershock deployment
 - 6,608 events with 94,280 P and 64,852 S arrivals
 - Aftershocks focus in bands and clusters.

- Synthetic models created of 12 km checkers with +5% perturbations
- Recovery of synthetic checkerboard shows good resolutions at the 12 km-scale, with some smearing of features, particularly toward the edges of the resolvable area.
- Best resolution in top ~35 km.

3. Geologic setting and Relocated Seismicity

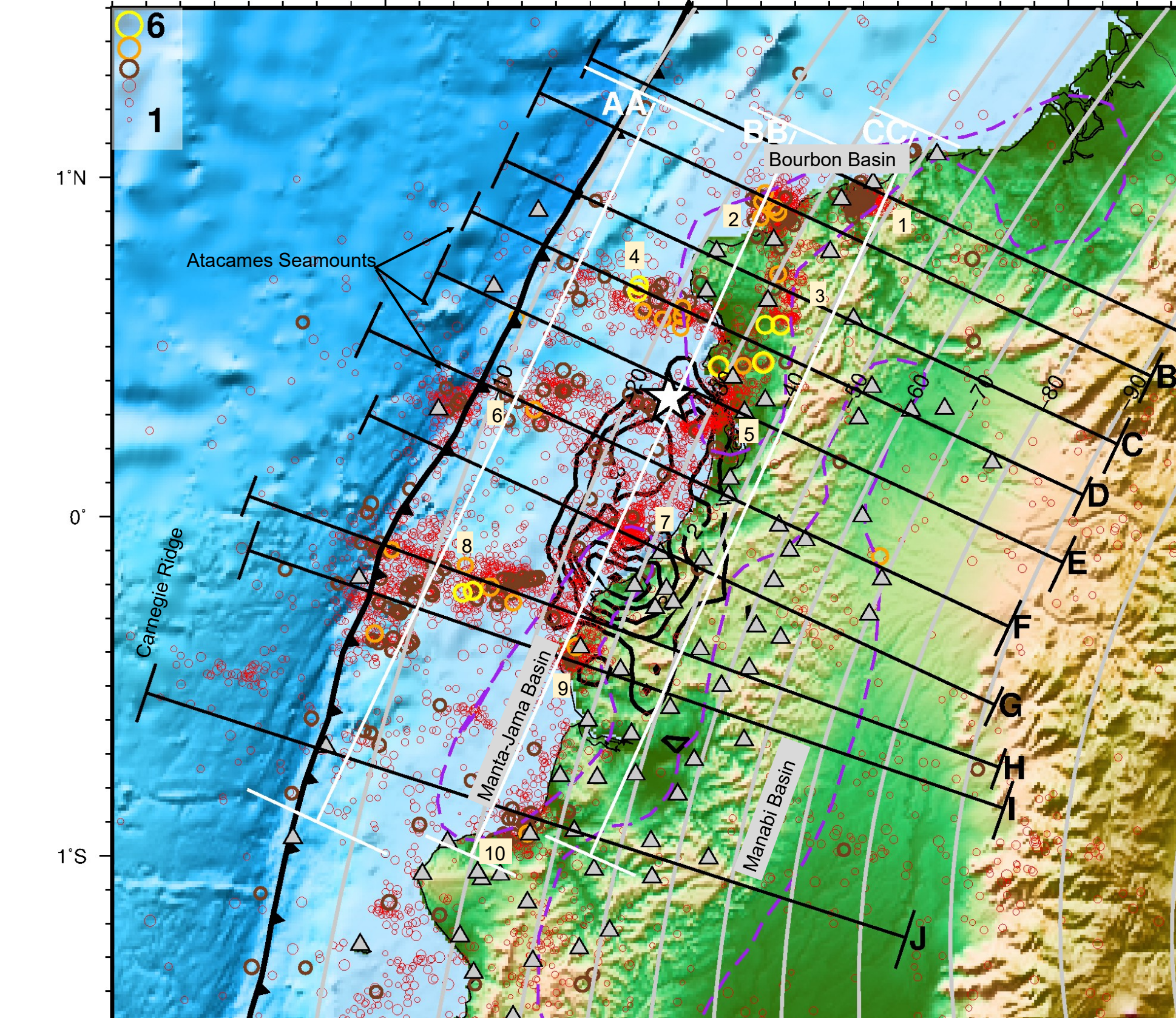
- Cretaceous-age accreted oceanic terranes underlie much of the north Ecuador forearc (shown in green in the map and cross sections below). They outcrop as the Piñon Formation, and are rigid material. Such material would be evidenced as fast velocities in the velocity model.
- Deep sedimentary basins are along the forearc (shown in purple dashed outlines), and are expected to be seen as low velocity features.
- Clusters of relocated aftershock seismicity are focused on the boundaries of the Bourbon Basin (northern basin) and Manta-Jama Basin (southern basin) and the uplift to the east. Two of the clusters along the Bourbon Basin coincide with a junction of north-south faults with northeast-southwest faults.



- Esmeraldas swarm in upper plate
- Suggestion of high Vp forearc terrane, but resolution is limited
- Atacames swarm in upper plate
- Seismicity at edge of high Vp/Vs feature aligning with basin
- High velocity forearc terrane better resolved
- Main seismicity in lower plate
- Seismicity at edge of and within high Vp/Vs feature aligning with basin
- Main seismicity interface & upper plate. Seismicity in lower plate on west side of section.
- Interface seismicity follows Font et al. 2013 slab
- Seismicity at edge of high Vp/Vs feature aligning with basin
- High Vp beneath Coastal Ranges and along accreted forearc terrane.
- Main seismicity beneath high Vp/Vs feature at edge of and within rupture
- Main seismicity locates between slab models and along Font et al. 2013 slab model.
- Seismicity focused within rupture area (between patches of greater slip) along interface and in upper and lower plates.
- Low Vp beneath Manabi Basin.
- High Vp/Vs feature within/above rupture and within Manabi Basin.
- High Vp feature within rupture area
- Rupture termination down dip at high Vp forearc terrane
- High Vp & Vp/Vs below Coastal Ranges
- Subducting Atacames seamounts appear as high Vp, low Vp/Vs features.
- Subducting topography on Carnegie ridge appears as high Vp.
- Subducting topography (on Carnegie Ridge and Atacames Seamounts) focusses seismicity primarily at plate interface and in lower plate.
- Seismicity focused around subducting topography (high Vp) in lower and upper plates.
- Termination of Pedernales rupture at subducted topography (updip) and high Vp forearc terrane (down dip).
- High Vp/Vs within rupture area/basin areas.
- High Vp within rupture area.
- Seismicity focused around subducting topography (high Vp) in lower and upper plates
- Pedernales rupture termination down dip at forearc terrane
- Low Vp aligned with Manabi Basin
- High Vp/Vs aligned with Jama Basin and rupture area, but not Manabi Basin
- Main seismicity in lower plate down dip of high velocity feature.
- Low Vp/Vs beneath southern end of Jama basin.
- Low Vp beneath Manabi basin.
- High Vp/Vs in region of lower slip within Pedernales rupture area
- High Vp/Vs aligning with basins and edge of rupture area.
- Within rupture area, seismicity mostly locates along and between two plate interface models.
- Low Vp/Vs at edge of Jama Basin where seismicity is focused.
- Low Vp and high Vp/Vs feature at down dip edge of Pedernales rupture.
- High Vp/Vs along edges of basins.
- Seismicity primarily at or above plate interface as modeled by Font et al. 2013.

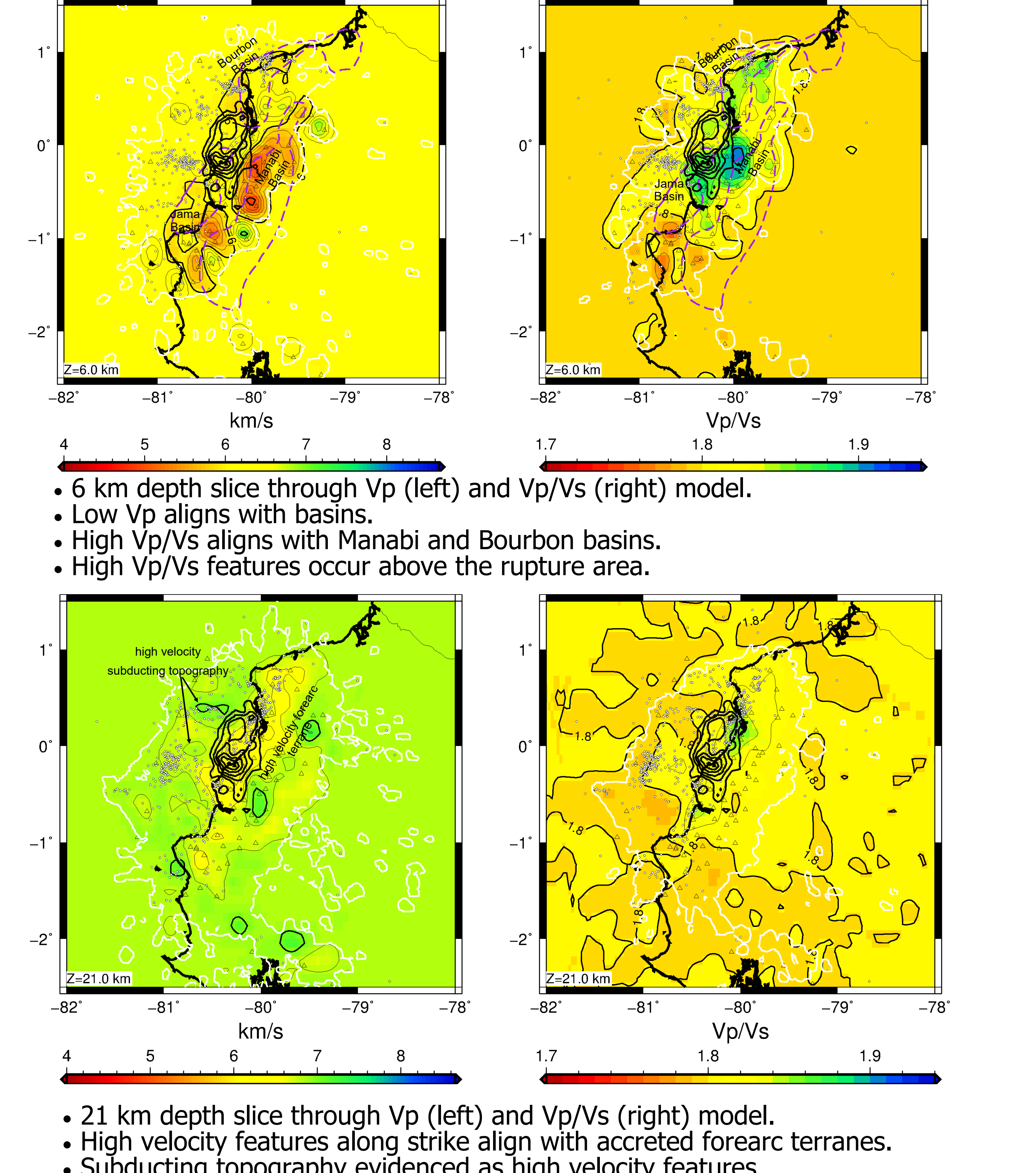
4. Joint Inversion for Earthquake Relocation and Velocity Model

- Relocation of earthquakes in the joint inversion results in bands of seismicity collapsing to discrete clusters (for comparison, see section 2).
- Clusters co-locate with clustering in interseismic seismicity (section 1).
- Clusters of seismicity (numbered 1, 3, 9, and 10) locate along the boundary between basins and the Coastal Ranges.
- Clusters of seismicity outline the subducting Atacames Seamounts (6) and subducting topography on the Carnegie Ridge (8).
- The cluster within the rupture area between the patches of greater slip (7) became more focused in the relocation, as did the cluster on the north side of the rupture (5).
- Clusters 1 and 2 consist of upper plate events, mostly occurring within swarms.



Cross sections through velocity model shown below. Events ML 4+ shown as black circles on cross sections. White contour marks region with 10+ rays (resolvable).

Sedimentary basins shown in purple dashed lines (Reyes 2013). Pedernales mainshock (white star) and rupture (black contours of coseismic slip) from Nocquet et al. (2017). Stations are gray triangles. Slab 2.0 (Hayes, 2018) isodensity contours shown in gray.



- 6 km depth slice through Vp (left) and Vp/Vs (right) model.
- Low Vp aligns with basins.
- High Vp/Vs aligns with Manabi and Bourbon basins.
- High Vp/Vs features occur above the rupture area.
- 21 km depth slice through Vp (left) and Vp/Vs (right) model.
- High velocity features along strike align with accreted forearc terranes.
- Subducting topography evidenced as high velocity features.

5. Conclusions

- Joint inversion for 3D velocity structure and earthquake location provides significantly improved precision in earthquake locations.
- Clusters in aftershock seismicity align with clusters in background seismicity.
- High velocity features are seen corresponding to accreted forearc terranes and subducting high topography.
- Sedimentary basins are seen as low velocity features. The Manabi and Bourbon Basins are seen as high Vp/Vs features.
- Subducted topography focuses seismicity.
- Limits of the Pedernales rupture align up-dip with subducted topography in the lower plate and down-dip with accreted forearc terranes in the upper plate.
- Existing features, including basins, accreted terranes, and subducting topographic features are expressed in the velocity model and control megathrust, postseismic, and interseismic deformation across megathrust cycles.

6. Acknowledgements

This work is supported by the NSF RAPID Program Award EAR-1642498 and NSF Geophysics Program Award EAR-1723042 and EAR-1723065. Additional instrumentation comes from Instituto Geofísico at the Escuela Politécnica Nacional (IG-EPN) in Quito Ecuador, L'Institut de recherche pour le développement (IRD) Géozaur in Nice France, and University of Liverpool UK, with financial support from IG-EPN, IRD, CNRS, and NERC.

Key References

- Nocquet, J.-M., Jarrin, P., Vallée, M., Mothes, P.A., Grandin, R., Rolandone, F., Delouis, B., Yepes, H., Font, Y., Fuentes, D., Régnier, M., Laurendeau, A., Cisneros, D., Hernandez, S., 2017. Supercycle at the Ecuadorian subduction zone revealed after the 2016 Pedernales earthquake: Nature Geoscience, v. 1, no. December, p. 1–8, doi: 10.1038/ngeo2864
- Font, Y., Segovia, M., Vaca, S., Theunissen, T., 2013. Seismicity patterns along the Ecuadorian subduction zone: New constraints from earthquake location in a 3-D a priori velocity model. Geophys. J. Int. 193, 263–286. https://doi.org/10.1093/gji/ggs083
- Roecker, S., Thurber, C., Roberts, K., and Powell, L., 2006. Refining the image of the San Andreas Fault near Parkfield, California using a finite difference travel time computation technique: Tectonophysics, v. 426, no. 1–2, p. 189–205, doi: 10.1016/j.tecto.2006.02.026.